Environmental Science
Processes & Impacts

PAPER

View Article Online
View Journal

Cite this: DOI: 10.1039/c6em00037a

Sources of organic matter (PAHs and *n*-alkanes) in $PM_{2.5}$ of Beijing in haze weather analyzed by combining the C–N isotopic and PCA-MLR analyses

Xinyue Guo,[a] Cai Li,[a] Yang Gao,[a] Lei Tang,[a] Meryem Briki,[a] Huaijian Ding[a] and Hongbing Ji*[ab]

Organic molecular composition and carbon and nitrogen isotope ratios of $PM_{2.5}$ samples collected in November 2013 were analyzed using gas chromatography/mass spectrometry and isotope ratio mass spectrometry. The samples represented six potential sources and seven sampling sites situated in concentric zones around Beijing under both haze and non-haze conditions. Our results showed that the average concentrations of polycyclic aromatic hydrocarbons (PAHs) and *n*-alkanes were 258.2 ± 208.8 ng m^{-3} and 499.5 ± 347.8 ng m^{-3}, while the $\delta^{13}C$ and $\delta^{15}N$ values for $PM_{2.5}$ varied from −26.29 to −25.26‰ and from 8.68 to 14.50‰ with an average of −25.70 ± 0.3‰ and 11.97 ± 1.79‰, respectively. The highest concentrations of PAHs and *n*-alkanes were recorded in the sixth ring road, with the lowest ones in the third ring road. Concentrations of PAHs during haze were higher than during non-haze conditions, while concentrations of *n*-alkanes were not markedly different. Principal component analysis/multiple linear regression analyses indicated that the main sources of PAHs were vehicle and coal combustion emissions, while *n*-alkanes had high contributions from petroleum emissions. These sources were supported by isotopic analyses. Thus, the main sources of organic matter contributing to haze in Beijing were coal combustion and vehicle emissions. Such results provide guidance towards managing haze in Beijing.

Received 24th January 2016
Accepted 23rd February 2016

DOI: 10.1039/c6em00037a

rsc.li/process-impacts

Environmental impact

Beijing, the capital of China, has experienced serious air pollution of fine particulate matter in recent years. Organic molecular composition and carbon and nitrogen isotope ratios of $PM_{2.5}$ samples were analyzed to identify the $PM_{2.5}$ sources under haze and non-haze conditions. The results of isotopic values were in agreement with those of organic molecular compositions, indicating that coal combustion and vehicle emissions were the major sources of organic matter contributing to haze in Beijing. This provides a new method for tracing the sources of $PM_{2.5}$.

1 Introduction

With the massive development of residential areas and industries around Beijing, China's capital is facing very serious air pollution problems. Studies of atmospheric particulate matter showed that the particle sizes ranged from 1 nm to 100 μm, spanning five orders of magnitude.[1,2] The inhalable particle component, with its large particle number and surface area, not only affects atmospheric visibility, but also endangers human health, causing morbidity and mortality.[3] Atmospheric particles are a complex mixture of components, including inorganic, organic, and biological materials.

Organic components of this particulate matter are of increasing interest, as they have the potential to play an important role in atmospheric chemistry and air quality. Polycyclic aromatic hydrocarbons (PAHs) behaving like persistent organic pollutants are of major concern for human health, because they are bioaccumulative, resist degradation, and can cycle in the environment for a long time.[4,5] PAHs, often with three to six rings, are produced mainly through incomplete combustion and pyrolysis of carbon-containing materials, such as fossil fuels and biomasses.[6] While *n*-alkanes are emitted by anthropogenic and natural sources, anthropogenic sources of *n*-alkanes typically include combustion of fossil fuels, wood, agricultural debris, or leaves. Biogenic sources include particles shed from the leaf epicuticular waxes of vascular plants and direct suspension of pollen, microorganisms, and insects.[7] Atmospheric studies of PAHs and *n*-alkane deposition have been carried out worldwide.[8–14]

[a]College of Civil and Environmental Engineering, University of Science and Technology Beijing, Beijing 100083, China. E-mail: ji.hongbing@hotmail.com; Fax: +86-10-68909710; Tel: +86-10-68909710

[b]The State Key Laboratory of Environmental Geochemistry, Institute of Geochemistry, Chinese Academy of Sciences, Guiyang 55002, China

To formulate effective control strategies and reduce the potential toxic effects of $PM_{2.5}$, an understanding of the sources of organic matter in the atmosphere is required. Both PAHs and *n*-alkanes contain useful markers for source identification of fine particles (Bi *et al.*, 2002; Simoneit, 1986).[7,15] In fact, some particle-phase PAHs and *n*-alkanes have been used as chemical mass balance models for $PM_{2.5}$ source apportionment.[16–18] In addition, isotopic analysis is an effective method for distinguishing the sources of organic carbon (OC). Carbon isotope and nitrogen isotope ratios are used to distinguish individual dominant sources of atmospheric pollution.[19–22]

Stable carbon isotopes (^{13}C and ^{12}C) have proven to be very useful for tracing sources; these isotopes were first applied to studies of air pollution in the 1980s.[23] Several authors[24–26] explored the use of carbon isotopes in organic carbon for source apportionment and atmospheric chemical transformation studies. Cao *et al.*[27] used stable carbon isotope ratios to determine that the carbonaceous component of $PM_{2.5}$ was derived from fossil fuels, especially coal combustion and motor vehicle emissions. They showed that cities in North China were strongly affected by coal combustion during winter. Studies of nitrogen isotopes (^{15}N and ^{14}N) are fewer,[28–30] but still could have potential as tracers. Widory[31] measured $\delta^{15}N$ in the atmosphere of Paris; these measurements provided clear information on the sources of primary and possibly secondary nitrogen from road traffic, waste incinerators, and heating sources. Thus, it was possible to characterize emissions from different types of emitters in Paris.

However, few studies combine organic molecular composition with isotope ratios to ascertain sources of particles during haze. In this study, the concentrations of PAHs and *n*-alkanes in $PM_{2.5}$ samples collected during haze and non-haze conditions were measured using gas chromatography coupled with mass spectrometry and analyzed using principal component analysis (PCA) and multiple linear regression (MLR) methods to determine their sources. At the same time, six potential sources of $PM_{2.5}$ were collected and the carbon and nitrogen isotope ratios of these sources were compared with the ratios of our samples to establish their origins.

2 Materials and methods

2.1 Sampling

$PM_{2.5}$ samples were collected at seven sites within concentric zones around Beijing, the capital of China. From the second loop to Miyun county, seven sample sites were set in each ring

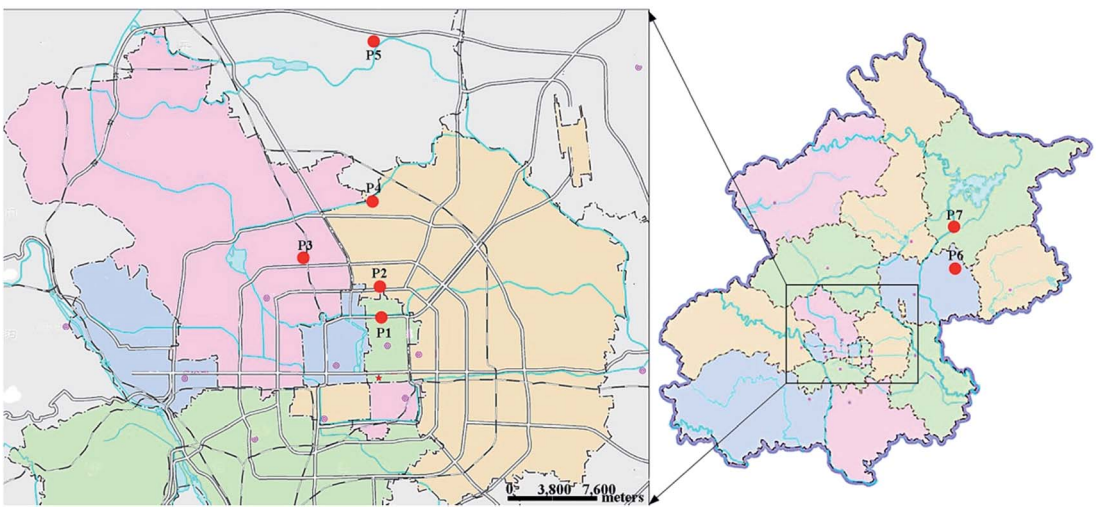

Fig. 1 Distribution of sample sites in Beijing.

Table 1 The location of the sample sites

No.	Location	Latitude (N)	Longitude (E)	Sampling date	
				Haze	Non-haze
P1	2nd ring road	39° 56′ 48.00″	116° 24′ 02.86″	11.5.2013	12.3.2013
P2	3rd ring road	39° 58′ 11.34″	116° 24′ 06.64″	12.7.2013	11.6.2013
P3	4th ring road	39° 59′ 14.76″	116° 21′ 13.18″	12.6.2013	11.10.2013
P4	5th ring road	40° 00′ 50.56″	116° 24′ 34.29″	12.7.2013	11.7.2013
P5	6th ring road	40° 09′ 22.86″	116° 26′ 22.00″	11.12.2013	—
P6	Shunyi district	40° 11′ 22.94″	116° 52′ 40.11″	11.15.2013	11.13.2013
P7	Miyun county	40° 21′ 46.51″	116° 49′ 27.50″	11.23.2013	11.14.2013

road, Shunyi district and Miyun county (Fig. 1 and Table 1). Using a median volume sampler with $PM_{2.5}$ cutting equipment (manufactured by Laoying, Qingdao, China), $PM_{2.5}$ samples were collected on quartz filters (with 88 mm diameter). Each sample was collected for 24 hours with a flow rate of 100 L min^{-1}. The sampler was placed more than 20 m away from the main area of human activity and about 1.5 m above the ground. Samples were collected under both haze and non-haze conditions during Nov–Dec 2013 (Table 1). In addition, six source samples were collected under the same conditions from biomass combustion, anthracite combustion, diesel exhaust, automobile exhaust, lampblack and road gas; the source samples were also collected by the median volume sampler under the same conditions (100 L min^{-1}, 24 h). Before sampling, the filters were baked at 450 °C for 8 h to remove volatile substances and organic contaminants, and then were stored at room temperature (25 °C) and under a relative humidity of 50% for 24 h before weighing. After sampling and weighing, the filters were wrapped in aluminum foil and stored in a refrigerator at −40 °C, prior to sampling.

2.2 Analytical methods

Details of the methods used for $PM_{2.5}$ sample extraction and our clean-up procedure can be found in a previous study;[32,33] a brief summary is given below. Aliquots of filter samples (1/4) were ultrasonically extracted three times for 15 min each with dichloromethane/methanol (1 : 1, v/v). After filtering, the solvent extracts were combined and concentrated on a rotary evaporator; the extract was reduced to 1 mL with dry nitrogen gas. Aliquots of these extracts were reacted with bis (trimethylsilyl)-trifluoroacetamide (BSTFA), containing 1% trimethyl-chlorosilane and pyridine for 3 h at 70 °C to derivatize –COOH and –OH groups to their corresponding trimethylsilyl esters and ethers, respectively. The silylated extracts were dried with N_2 to remove the remaining BSTFA and pyridine, and then were added to *n*-hexane and internal standards before injection into the gas chromatograph.

An Agilent/HP 6890 gas chromatograph (GC; Agilent/Hewlitt-Packard, Santa Clara, CA, USA) equipped with a 30 m DB-5MS (0.25 mm i.d., 0.10 mm in thickness, J&W Scientific) capillary column coupled to a Micromass VG Platform II mass spectrometer (MS; Waters, Manchester, UK) operating in the electron impact mode (70 eV) was used to analyze the concentrations of 18 PAHs (naphthalene, acenaphthylene, acenaphthene, fluorene, phenanthrene, anthracene, fluoranthene, pyrene, retene, benz(*a*)anthracene, chrysene, benzo(*b*)fluoranthene; benzo(*k*)fluoranthene, benzo(*a*)-pyrene, 1,3,5-triphenylbenzene, indeno(1,2,3-*cd*)pyrene, dibenz(*a*,*h*)anthracene, and benzo(*g*,*h*,*i*)-perylene) and *n*-alkanes. Helium was used as the carrier gas at a flow rate of 1.5 mL min^{-1}. The injection was conducted in the splitless mode at 250 °C with an injection volume of 1 mL. The column temperature was started at 150 °C, maintained for 2 min, and ramped to 245 °C at 2 °C min^{-1}, held for 2 min, and then increased to 300 °C at 20 °C min^{-1}, and held for 5 min. GC-MS operated on a TSQ Quantum XLS system (Thermo Fisher Scientific, USA) in the scan mode was also employed to further identify the analytes in the samples. Data acquisition and processing were controlled by a HP Chemstation data system.

The statistical analysis using PCA and MLR analysis was carried out using IBM SPSS statistical software packages to extract the possible sources of PAHs and *n*-alkanes. In this study, PCA has been applied to identify sources of PAHs and *n*-alkanes in order to provide a further understanding of the haze conditions in Beijing. MLR analysis was applied to quantify source contributions to PAHs and *n*-alkanes in the atmosphere in Beijing. MLR was carried out with standardized component scores of PCs as independent variables and standardized total concentrations of PAHs and *n*-alkanes as dependent variables. Source contributions were estimated based on regression equations and regression coefficients.

2.3 Quality control (QC) and quality assurance (QA)

All data in the study were subject to strict quality-control procedures to minimize sampling/measurement errors. Samples were analyzed more than 3 times on different days to check for reproducibility and reduce measurement errors. A number of field and laboratory blanks were taken during sampling and processing. Blank samples were measured everyday under the same conditions as real samples. All compounds, but three recovery indicators, were under detection limits in blanks. The average recoveries of the three indicators were from 70 to 110% for the experimental process.

2.4 Isotope experiments

The contents of carbon, nitrogen, and their isotope ratios $\delta^{13}C$ and $\delta^{15}N$ of the aerosols were determined using an Isotope Ratio Mass Spectrometer (DELTA V Advantage; Thermo Fisher Scientific, Waltham, MA, USA) and an Elemental Analyzer (Flash EA1112 HT; Thermo Fisher Scientific). In the isotope experiments, the aliquots of sample filters (1/2) and CuO, Cu, and CaO were transferred to a quartz-glass tube and combusted at 900 °C within the Elemental Analyzer to convert C into CO_2 and N into N_2. The cooled gases were then analyzed in the Isotope Ratio Mass Spectrometer. Because measurements of the analysis blank (mainly caused by reactants) can vary slightly over time from 0.1 to 2 nmol, each series of three samples was analyzed together with a blank. Nitrogen was measured with an accuracy of 70.5% (2 s), estimated from the reproducibility measurements of the international standards.

Variations in the isotopic composition of the bulk carbon (‰, *vs.* V-PDB) and nitrogen (‰, *vs.* standard atmospheric N_2) in samples are expressed in the usual δ notation. The $\delta^{13}C$ and $\delta^{15}N$ measurements had an overall precision of ±0.1‰ and ±0.2‰, respectively.

$$\delta^{13}C_{sample}\ (‰) = \left[\frac{\left(^{13}C/^{12}C\right)_{sample}}{\left(^{13}C/^{12}C\right)_{standard}} - 1\right] \times 10^3 \quad (1)$$

$$\delta^{15}N_{sample}\ (‰) = \left[\frac{\left(^{15}N/^{14}N\right)_{sample}}{\left(^{15}N/^{14}N\right)_{standard}} - 1\right] \times 10^3 \quad (2)$$

3 Results and discussion

3.1 Pollution from the PAHs and *n*-alkanes

3.1.1 PAH concentration. Eighteen PAHs were detected in the $PM_{2.5}$ samples, although naphthalene and acenaphthene were not detected in all samples; the concentrations of the other 16 PAHs are presented in Fig. 2. The average concentrations of individual 16 PAHs varied from 1.1 to 37.3 ng m^{-3}, while the concentration of their sum ($\sum$16PAHs) ranged from 36.8 to 479.8 ng m^{-3}, with a mean of 258.2 ± 208.8 ng m^{-3}. These results were about 5–10 times higher than those for summer in Guangzhou, a city in the south of China, but only 2–3 times those for winter.[34] They were also much higher than those measured in Harbin, a city in northeast China.[35] The mean concentrations of PAHs in this study were 50% higher than those recorded from January to March 2006,[36] and 2–3 times the values for September 2008 and July 2009.[37]

In Fig. 2, higher ring PAHs (with four to six rings) were the dominant species, with fluoranthene, pyrene, benz(*a*)anthracene (BaA), chrysene, benzo(*b*)fluoranthene (BbF), benzo(*k*)fluoranthene (BkF), and benzo(*a*)pyrene (BaP) constituting more than 90% of the $\sum$16PAHs. This result was consistent with other studies.[34,37,38]

Comparison of the concentrations of $\sum$16PAHs for each site under both haze and non-haze conditions (Fig. 2) shows that the concentrations in haze were higher, except for the Miyun county site. Interestingly, the minimum concentration in non-haze samples was 36.8 ng m^{-3} in the fourth ring road, similar to concentrations in Guangzhou in winter;[34] while the maximum was 287.3 ng m^{-3} in Miyun county. The range of concentrations under non-haze conditions (36.8–287.3 ng m^{-3}) was a little higher than for Beijing in 2009.[39] The concentrations of haze samples were very high, ranging from 126.6 to 479.8 ng m^{-3}, about 2–3 times the values under non-haze conditions. This result suggests that under non-haze conditions, the air quality in Beijing is comparable to other Chinese cities, but during hazy days, the air pollution is serious.

3.1.2 *n*-Alkane concentrations. The concentrations or *n*-alkanes with C12 to C36 are shown in Fig. 3. The content of $\sum$*n*-alkanes varied between 168.0 and 901.6 ng m^{-3}, with an average concentration of 499.5 ± 347.8 ng m^{-3}. These results were similar to those recorded in Guangzhou for April, but higher than summer values in Guangzhou.[8] Likewise, they are 2–3 times those for Beijing from 2006.[40] The major contributors to $\sum$*n*-alkanes were the lighter congeners (C13 and C19–C25), accounting for 39.3–50.3% of the total sum. The highest concentrations were recorded in the sixth ring road, followed by the Shunyi district, fourth ring road, second ring road, Miyun county, and third ring road, in decreasing order.

The differences between samples collected under haze and non-haze conditions were different from those for PAHs. Concentrations for haze were higher than those for non-haze conditions in the second to fourth ring roads. While in the fifth ring road, Shunyi district, and Miyun county, non-haze samples were higher than haze ones. Such differences likely reflect different sources.

The carbon preference index (CPI) of *n*-alkanes is used to calculate the contributions of biogenic *versus* fossil fuel combustions.[41,42] We defined CPI1 as the average CPI for the whole range of *n*-alkanes (C12–C36), while CPI2 denotes only petrogenic *n*-alkanes (C12–C25), and CPI3 (C25–C36) gives values for biogenic-*n*-alkanes. Their values were 0.99, 1.16, and

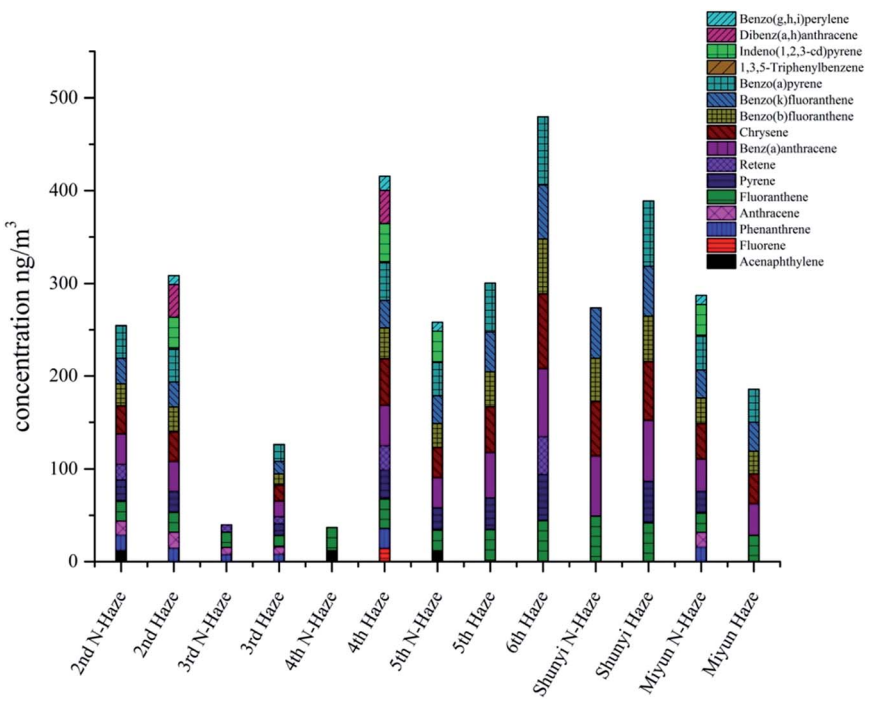

Fig. 2 Concentrations of PAHs in $PM_{2.5}$ samples.

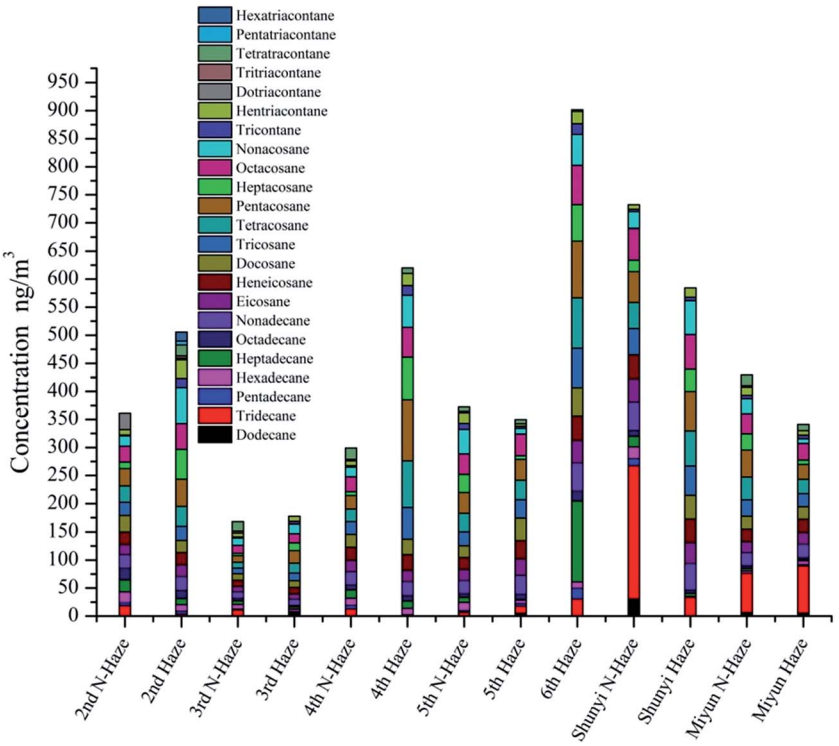

Fig. 3 Concentrations of *n*-alkanes in $PM_{2.5}$ samples.

0.82, respectively. The CPI values show that *n*-alkanes were derived from high contributions of petroleum, diesel residues, and gasoline emissions, with a minor contribution of *n*-alkanes emitted from plant waxes.

$$\mathrm{CPI1} = \frac{\sum \mathrm{C13-C36}}{\sum \mathrm{C12-C35}} \quad \mathrm{CPI2} = \frac{\sum \mathrm{C13-C25}}{\sum \mathrm{C12-C24}}$$
$$\mathrm{CPI3} = \frac{\sum \mathrm{C25-C36}}{\sum \mathrm{C24-C35}} \qquad (3)$$

3.2 PCA-MLR analysis and the sources of PAHs and *n*-alkanes

In the beginning, the Positive Matrix Factorization (PMF) model was used to analyze the sources of organics in the atmosphere, but the results were uncertain in 4, 5 or more factors, so it is hard to determine the sources of PAHs and *n*-alkanes. The reason for this phenomenon was that the samples were collected in different places and weather conditions, and thus their main sources were not similar to each other. PCA is a reliable model for identifying the sources of organics in the atmosphere.[35,43] Here, PCA was used to identify the sources of PAHs and *n*-alkanes in Beijing. Five principal components (PCs) explained 91.9% of the total variance in PAHs (Table 2). The first component (PC1) accounted for 39.2%, and was mostly associated with four- and five-ring PAHs, such as fluoranthene, pyrene, benz(*a*)anthracene, chrysene, benzo(*b*)fluoranthene, benzo(*k*)fluoranthene, and benzo(*a*)pyrene. According to the literature, fluoranthene, pyrene, benz(*a*)anthracene, and chrysene are markers for coal combustion, while fluoranthene, pyrene, benzo(*b*)fluoranthene, and benzo(*k*)fluoranthene are tracers for vehicle emissions, and benz(*a*)anthracene is a tracer for natural gas combustion.[6,44] Thus, PC1 reflected combustion of fossil fuels. The second component (PC2) was enriched in fluorene, phenanthrene, 1,3,5-triphenylbenzene, indeno(1,2,3-*cd*)pyrene, dibenz(*a*,*h*)-anthracene, and benzo(*g*,*h*,*i*)perylene, accounting for 30.4% of the total variance in PAHs (Table 2).

Table 2 PCA results of PAHs

	Component				
PAHs	PC1	PC2	PC3	PC4	PC5
Acenaphthylene	−0.385	−0.136	0.056	0.290	0.767
Fluorene	0.120	**0.703**	−0.596	0.258	−0.074
Phenanthrene	−0.273	**0.810**	0.181	0.214	−0.279
Anthracene	−0.420	0.390	**0.729**	−0.054	−0.274
Fluoranthene	**0.851**	−0.222	−0.323	−0.153	−0.026
Pyrene	**0.741**	0.323	0.341	0.285	0.204
Retene	0.419	0.268	−0.092	**0.780**	−0.175
Benz(*a*)anthracene	**0.973**	0.032	0.045	−0.138	−0.021
Chrysene	**0.985**	0.114	0.032	−0.045	−0.021
Benzo(*b*)fluoranthene	**0.979**	0.066	0.070	−0.122	−0.010
Benzo(*k*)fluoranthene	**0.955**	−0.035	0.099	−0.205	0.017
Benzo(*a*)pyrene	**0.775**	0.200	0.356	0.190	0.177
1,3,5-Triphenylbenzene	−0.148	**0.930**	0.068	−0.197	0.097
Indeno(1,2,3-*cd*)pyrene	−0.071	**0.892**	−0.018	−0.248	0.282
Dibenz(*a*,*h*)anthracene	−0.003	**0.869**	−0.212	−0.098	−0.153
Benzo(*g*,*h*,*i*)perylene	−0.045	**0.920**	−0.111	−0.183	0.244
Explained variance (%)	39.2	30.4	8.5	7.3	6.4

These higher ring PAHs are tracers of gasoline-powered vehicles (Harrison *et al.*, 1996). Thus, PC2 reflected the use of gasoline-powered vehicles. The third component (PC3), with 8.5% of the total variance, is associated with anthracene, and also pyrene and benzo(*a*)pyrene; these three PAHs are coal combustion tracers.[6] Thus, PC3 reflected coal combustion emissions. Components PC4 and PC5, enriched in retene and acenaphthylene, comprised 7.3% and 6.4% of the total variance, respectively. Retene is produced from the combustion of coniferous wood, while acenaphthylene is the tracer for cement plant emissions.[44–46]

Table 3 gives PCA results of *n*-alkanes. Four PCs explained 85.0% of the total variance. PC1 was highly loaded with C15 and C17–C31 *n*-alkanes, accounting for 42.0% of the total variance. PC2 had a high loading of C29–C31 and C33–C36, accounting for 21.2% of the total variance. PC3 was characterized by a high loading of the short-chain *n*-alkanes (C12–C16), representing 11.5% of the total variance, while PC4 was highly loaded with C18 and C32, accounting for 10.3% of the total variance. According to the literature, C12–C25 are derived from fossil fuel burning, including vehicle emissions and coal burning; while C26–C36 have a biogenic source and are derived from higher plant waxes.[47,48] Thus, PC1 reflected fossil fuel burning and plant waxes, PC2 was directly derived from higher plant waxes, PC3 reflected vehicle emissions and coal burning, while PC4 also reflected both fossil fuel burning and higher plant waxes.

MLR analysis was used to quantify source contributions to samples based on PAHs and *n*-alkanes. MLR was carried out using the standardized component scores of PCs as independent variables and the standardized total concentrations of PAHs and *n*-alkanes as dependent variables. Regression coefficients were used to estimate source contributions. Eqn (4) and (5) describe the PCs' contributions of PAHs and *n*-alkanes to samples.

$$\sum 16\text{PAHs} = 0.886\text{PC1} + 0.440\text{PC2} + 0.114\text{PC3} + 0.035\text{PC4} + 0.060\text{PC5} \quad (4)$$

$$\sum n\text{-Alkanes} = 0.967\text{PC1} - 0.08\text{PC2} + 0.171\text{PC3} - 0.096\text{PC4} \quad (5)$$

For PAHs, the contributions of PC1 (fossil fuels), PC2 (gasoline-powered vehicles), PC3 (coal combustion emissions), PC4 (coniferous wood combustion), and PC5 (cement plant emissions) were 58%, 29%, 7%, 2%, and 4%, respectively. Our analyses indicated that coal combustion and gasoline-powered vehicles were the dominant PAH sources, accounting for more than 85% of their contribution to the atmosphere. For *n*-alkanes, PC1 (fossil fuel burning and higher plant waxes) and PC3 (vehicle emissions and coal burning) were the dominant sources, contributing 85% and 15% of the total. PC2 and PC4 were close to zero, suggesting that their contributions were negligible.

Both data analyses show that the main sources of PAHs and *n*-alkanes in winter in Beijing were coal combustion emissions and vehicle emissions. This is consistent with the fact that coal is the main energy source in North China, especially in winter when there is a need for heating[49–51] Motor vehicles in Beijing already are related to high PM pollution problems.[52] Recent increases in both energy consumption and private vehicle ownership have aggravated air pollution in recent years.[53]

Table 3 PCA results of *n*-alkanes

	Component			
n-Alkanes	PC1	PC2	PC3	PC4
Dodecane (C_{12})	0.072	−0.660	**0.578**	−0.390
Tridecane (C_{13})	0.191	−0.656	**0.567**	−0.372
Pentadecane (C_{15})	**0.687**	−0.271	0.320	0.281
Hexadecane (C_{16})	0.162	−0.172	**0.706**	0.445
Heptadecane (C_{17})	**0.711**	−0.029	−0.055	0.349
Octadecane (C_{18})	0.564	0.099	0.331	**0.723**
Nonadecane (C_{19})	**0.830**	−0.403	0.139	−0.126
Eicosane (C_{20})	**0.812**	−0.412	0.146	−0.180
Heneicosane (C_{21})	**0.857**	−0.385	0.044	−0.152
Docosane (C_{22})	**0.568**	0.151	−0.599	0.305
Tricosane (C_{23})	**0.963**	−0.136	−0.155	−0.102
Tetracosane (C_{24})	**0.938**	0.052	−0.229	−0.077
Pentacosane (C_{25})	**0.907**	0.135	−0.189	−0.115
Heptacosane (C_{27})	**0.784**	0.507	−0.083	−0.118
Octacosane (C_{28})	**0.968**	−0.025	0.050	−0.186
Nonacosane (C_{29})	**0.741**	0.538	0.040	−0.173
Tricontane (C_{30})	**0.706**	0.590	−0.020	−0.072
Hentriacontane (C_{31})	0.543	**0.792**	0.163	−0.072
Dotriacontane (C_{32})	−0.018	−0.076	0.165	**0.886**
Tritriacontane (C_{33})	−0.405	**0.641**	0.326	−0.151
Tetratracontane (C_{34})	−0.435	**0.569**	0.141	−0.261
Pentatriacontane (C_{35})	0.077	**0.737**	0.539	−0.050
Hexatriacontane (C_{36})	0.077	**0.737**	0.539	−0.050
Explained variance (%)	42.0	21.2	11.5	10.3

3.3 Isotope composition

The samples from six potential sources and seven sampling sites were analyzed by isotope ratio mass spectrometry. Although the results of road gas were similar with those of the sampling sites, it could not be considered as a kind of source. Thus, only five potential sources were discussed.

3.3.1 Carbon isotope in $PM_{2.5}$. The $\delta^{13}C$ (−27.55‰) of particles derived from burning firewood is comparable to that for C3 plants (−27.12‰) in Miyun county, Beijing (Lu *et al.* 2013). This $\delta^{13}C$ value is higher than the value obtained in Yurihonjo, Japan, where $\delta^{13}C$ values varied from −34.7‰ to −28.0‰.[54] The $\delta^{13}C$ of coal-combustion particles (−23.31‰) is similar to that for Chinese coal (−23.4 ± 1.2‰),[55] Parisian coal (−26 ± 0.5‰),[19] and Japanese coal from Yurihonjo (−23.3‰).[56] The $\delta^{13}C$ values for diesel (−25.90‰) and gasoline (−25.27‰) were within the same range as for Hangzhou, China (−28 to −26‰ for diesel and −27.6 to −23.5‰ for gasoline),[57] but slightly lower than values for Yurihonjo (−24.4‰ for diesel and −24.3‰ for gasoline). The $\delta^{13}C$ values for soot derived from diesel and gasoline were lower than for coal, consistent with studies.[56,58]

The $\delta^{13}C$ values and carbon concentrations for major emission sources and $PM_{2.5}$ samples are plotted in Fig. 4a. The carbon isotopic compositions of $PM_{2.5}$ samples varied from

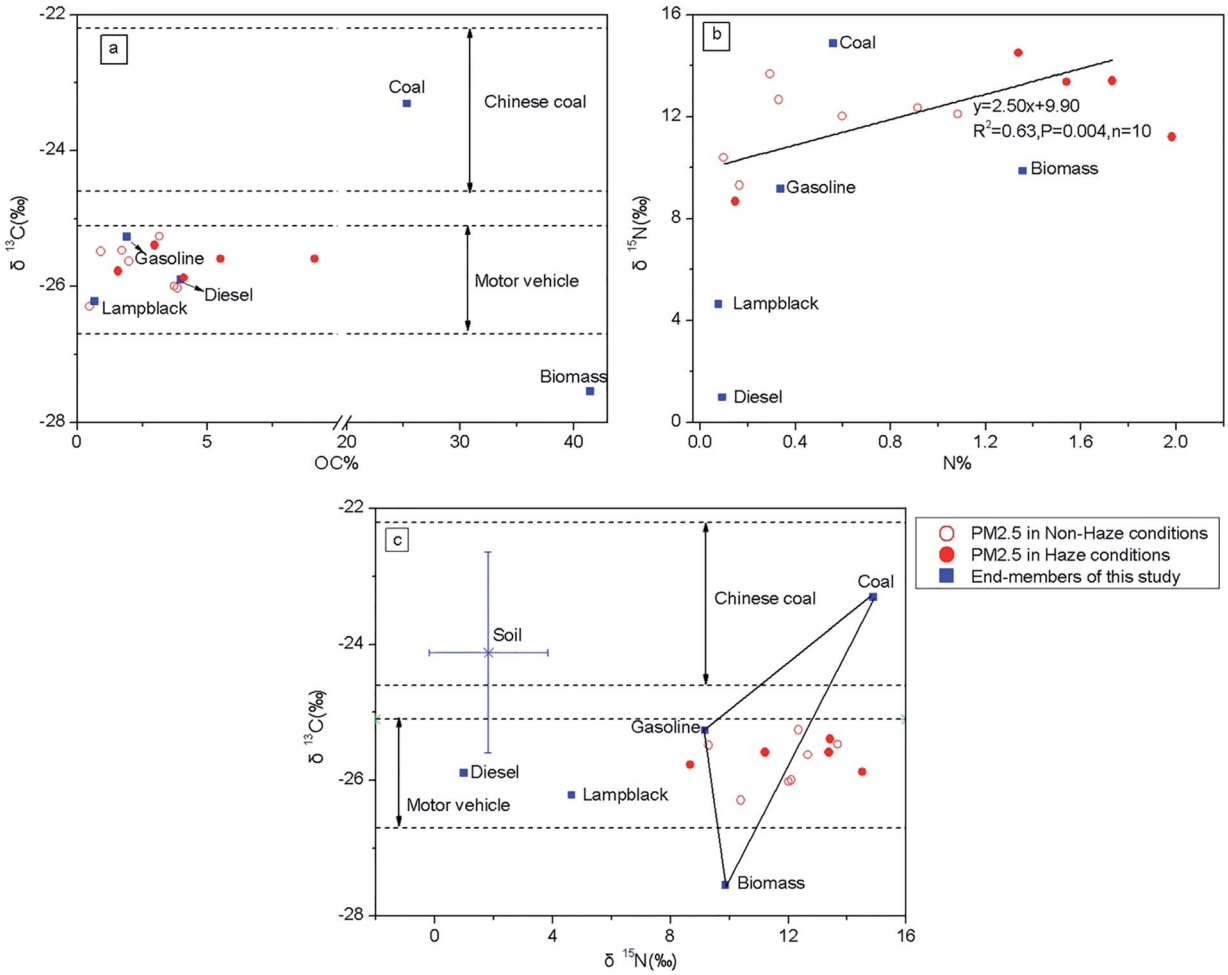

Fig. 4 Variations of $\delta^{13}C$ *vs.* OC% (a), $\delta^{15}N$ *vs.* N% (b) and $\delta^{13}C$ *vs.* $\delta^{15}N$ (c) in Beijing city. The dashed lines in (a and c) indicate the end-member $\delta^{13}C$ range of motor vehicles ($-25.9 \pm 0.8‰$)[62] and Chinese coal ($-23.4 \pm 1.2‰$).[55] The $\delta^{13}C$ and $\delta^{15}N$ values of the soil end member in (c) are taken from the study of Lu[63] in the Miyun watershed, Beijing.

-26.29 to $-25.26‰$, with an average of $-25.70 \pm 0.3‰$. The major emission sources for carbon in $PM_{2.5}$ samples were clearly motor vehicles and lampblack. The highest carbon concentration (9.11%) was recorded in the suburban area, where individual households use coal and biomass for burning. Other potential sources such as dust from construction areas and desert sand from the desert were negligible, given the higher $\delta^{13}C$ values for these end members (-17.5 to $-1.75‰$).[59] The contributions from motor vehicles and lampblack were estimated using a carbon isotopic mass balance equation. Because gasoline was the major vehicle fuel, it was used as the mixing end member. The results indicate that motor vehicles were the major emission source for carbon in $PM_{2.5}$ samples, with an average contribution of 57%. Motor vehicle pollution has become increasingly prominent, with the rapid urbanization in Beijing, while traditional use of coal and biomass burning has decreased under a series of clean air programs.

In Fig. 4a, the difference of $\delta^{13}C$ values under haze and non-haze conditions was not significant, showing that the carbon sources of $PM_{2.5}$ in haze weather were similar to those under non-haze conditions. However, compared with non-haze conditions, the carbon concentrations in haze were obviously higher. The results indicate that the sources of organic matter under haze and non-haze conditions were similar, but the atmospheric pollution in haze weather was more serious than under non-haze conditions.

3.3.2 Nitrogen isotope in $PM_{2.5}$. Nitrogen in atmospheric particles can be derived from multiple sources, including primary and secondary processes, making it difficult to identify its sources. Nitrogen isotopic composition ($\delta^{15}N$) can be useful for the identification of primary and secondary nitrogen.[31] The $\delta^{15}N$ values and nitrogen concentrations of major pollution sources and $PM_{2.5}$ samples are shown in Fig. 4b. The $\delta^{15}N$ values for $PM_{2.5}$ samples ranged from 8.68 to 14.50‰, with an average of $11.97 \pm 1.79‰$. The wide range of $\delta^{15}N$ values in $PM_{2.5}$ samples indicates multiple origins of nitrogen in the atmosphere or different processes of formation. This is similar to the values reported by the study[31] in Paris, where $\delta^{15}N$ (PM_{10}) ranged from 5.3 to 16.1‰, with an average of $10.7 \pm 3.1‰$. The $\delta^{15}N$ of coal in China ranged from -6 to $+4‰$,[60] while the $\delta^{15}N$ of NO_x from coal combustion ranged from 6 to 13‰.[61] The $\delta^{15}N$ values for diesel and gasoline were 0.98‰ and 9.17‰,

respectively. These values were different from those for Paris, where average $\delta^{15}N$ values for diesel and unleaded gasoline were both 4.6‰. Hence, the higher $\delta^{15}N$ values for $PM_{2.5}$ samples in Beijing may reflect the NO_x input from coal combustion. The nitrogen concentrations and $\delta^{15}N$ values in $PM_{2.5}$ samples showed a positive correlation ($R^2 = 0.63$, $P = 0.004$, with the exception of two samples), suggesting the formation of secondary nitrogen, as reported by Widory.[31] However, most of the nitrogen concentrations in $PM_{2.5}$ samples were similar to those measured directly at pollution sources, inferring that the influence of secondary processes is weak. In this case, a positive relationship between nitrogen concentrations and $\delta^{15}N$ values may indicate mixing of multiple pollution sources.

Plotting both $\delta^{13}C$ and $\delta^{15}N$ for $PM_{2.5}$ samples shows that gasoline, coal, and biomass combustion were the major sources of carbon and nitrogen in $PM_{2.5}$ samples (Fig. 4c). This varies slightly from the carbon source identification using $\delta^{13}C$ and carbon concentrations. However, the significant positive correlation ($R^2 = 0.52$, $P = 0.005$) between carbon and nitrogen concentrations in $PM_{2.5}$ samples suggests they had common pollution sources. Both isotopes and concentrations of carbon and nitrogen suggested that motor vehicles were an important pollution source of $PM_{2.5}$.

Although being similar to the results of the carbon isotope, there were a few differences between the $\delta^{15}N$ values under haze and non-haze conditions, and the nitrogen concentrations under haze conditions were three times that in non-haze weather. This result shows that there is more serious atmospheric pollution under haze conditions, but the pollution matter was from similar sources.

In summary, the results of isotopic analysis were in agreement with the results of PAHs, *n*-alkanes and PCA-MLR, indicating that the main sources of organic matter in $PM_{2.5}$ were vehicle emissions and coal combustion emissions, but their concentrations were much higher under haze weather conditions.

4 Conclusions

There was serious air pollution in Beijing in winter: the concentrations of PAHs and *n*-alkanes ranged from 36.8 to 479.8 ng m^{-3} and 168.0 to 901.6 ng m^{-3}, with the average of 258.2 ± 208.8 ng m^{-3} and 499.5 ± 347.8 ng m^{-3}, respectively. These concentrations were much higher than other cities in China, especially under haze conditions. The highest concentration of PAHs and *n*-alkanes was both in the sixth ring road and the lowest one was in the third ring road, and the concentrations of PAHs under haze conditions were higher than that under non-haze conditions, except in Miyun county, but the difference of *n*-alkanes between haze and non-haze conditions was not very clear.

PCA-MLR and CPI analysis indicated that the main sources of PAHs were vehicle emissions and coal combustion emissions, and *n*-alkanes included high contributions of petroleum, diesel residues and gasoline emissions and minor contributions of *n*-alkanes emitted directly from epicuticular waxes. In addition, the isotopic analysis result showed that the sources of organic matter were coal combustion emissions, vehicle emissions and biomass combustion emissions, which was similar to the result of PCA-MLR analysis, proving that the main sources of organic matter in Beijing were coal combustion emissions and vehicle emissions.

Carbon and nitrogen isotope analysis indicated that coal combustion and vehicle emissions were the major sources of $PM_{2.5}$ in Beijing. These results were in agreement with those of PCA-MLR analysis, proving that the carbon and nitrogen isotope analysis is a reliable new method for tracing the sources of $PM_{2.5}$.

Our study shows that sources of organic matter in $PM_{2.5}$ samples collected under haze and non-haze conditions were similar, but concentrations of organic matter were higher during haze. This suggests that haze pollution in Beijing is caused by coal combustion and vehicle emissions. Isotopic analyses showed that the contribution of coal combustion during haze was higher than under non-haze conditions. Thus, coal combustion for heating in winter contributed greatly to haze pollution in Beijing. These results provide guidance for managing haze in Beijing.

Acknowledgements

We are grateful to Dr. Bi Xinhui and Dr. Ren Zhaofang about organic matters analysis of $PM_{2.5}$ samples. The authors appreciate Guangzhou Institute of Geochemistry, Chinese Academy of Sciences and Chinese Academy of Forestry for analyzing the samples in the paper. This work was jointly supported from the National Natural Science Foundation of China (Nos. 41173113, 41473122) and the Hundred Talents Programs of Chinese Academy of Science.

Notes and references

1 Y. C. Chan and R. W. Simpsion, *Atmos. Environ.*, 1997, **31**, 3773–3785.
2 C. S. Christoforou, L. G. Salmon and M. P. Hannigan, *J. Air Waste Manage. Assoc.*, 2000, **50**, 43–45.
3 M. Koch and M. Amann, *Airborne fine particulates in the environment: a review of health effect studies, monitoring data and emission inventories*, IIASA, Laxengurg, Austria, 2000.
4 T. Bartos, P. Cupr, J. Klánová and I. Holoubek, *Environ. Int.*, 2009, **35**(7), 1066–1071.
5 J. M. Delgado-Saborit, C. Stark and R. M. Harrison, *Environ. Int.*, 2011, **37**(2), 383–392.
6 R. M. Harrison, D. J. T. Smith and L. Luhana, *Environ. Sci. Technol.*, 1996, **30**, 825–832.
7 B. R. T. Simoneit, *Int. J. Environ. Anal. Chem.*, 1986, **23**, 207–237.
8 X. H. Bi, G. Y. Sheng, P. A. Peng, Y. J. Chen, Z. Q. Zhang and J. Fu, *Atmos. Environ.*, 2003, **37**, 289–298.
9 S. P. Wu, S. Tao, F. L. Xu, R. Dawson, T. Lan, B. G. Li and J. Cao, *Sci. Total Environ.*, 2005, **345**, 115–126.
10 T. Gocht, O. Klemm and P. Grathwohl, *Atmos. Environ.*, 2007, **41**, 1315–1327.

11 Y. Tasdemir and F. Esen, *Atmos. Environ.*, 2007, **41**, 1288–1301.
12 W. Wang, N. Jariyasopit, J. Schrlau, Y. Jia, S. Tao, T. W. Yu, R. H. Dashwood, W. Zhang, X. Wang and S. L. Simonich, *Environ. Sci. Technol.*, 2011, **45**, 6887–6895.
13 S. C. Zhang, W. Zhang, Y. T. Shen, K. Y. Wang, L. W. Hu and X. J. Wang, *Atmos. Res.*, 2008, **89**, 138–148.
14 M. J. Xie, P. H. Michael and C. B. Kelley, *Atmos. Environ.*, 2014, **95**, 355–362.
15 X. H. Bi, G. Y. Sheng, P. A. Peng, Y. J. Chen, Z. Q. Zhang and J. M. Fu, *Sci. Total Environ.*, 2002, **300**, 213–228.
16 J. J. Schauer, W. F. Rogge, L. M. Hildemann, M. A. Mazurek, G. R. Cass and B. R. T. Simoneit, *Atmos. Environ.*, 1996, **30**, 3837–3855.
17 M. Zheng, G. R. Cass, J. J. Schauer and E. S. Edgerton, *Environ. Sci. Technol.*, 2002, **36**, 2361–2371.
18 M. Zheng, L. G. Salmon, J. J. Schauer, L. Zeng, C. S. Kiang, Y. Zhang and G. R. Cass, *Atmos. Environ.*, 2005, **39**, 3967–3976.
19 D. Widory, S. Roy, Y. Le Moullec, G. Goupil, A. Cocherie and C. Guerrot, *Atmos. Environ.*, 2004, **38**, 953–961.
20 S. D. Kelly, C. Stein and T. D. Jickells, *Atmos. Environ.*, 2005, **39**, 6007–6011.
21 D. Lòpez-Veneroni, *Atmos. Environ.*, 2009, **43**, 4491–4502.
22 G. Maciej, Z. Elżbieta, M. Małgorzata, L. S. Dominika and O. M. Jędrysek, *Isot. Environ. Health Stud.*, 2012, **48**(2), 327–344.
23 R. Chesselet, M. Fontugne and P. Buat-Menard, *Geophys. Res. Lett.*, 1981, **8**, 345–348.
24 K. F. Ho, S. C. Lee and J. J. Cao, *Atmos. Chem. Phys.*, 2006, **6**, 4569–4576.
25 L. Huang, J. R. Brook and W. Zhang, *Atmos. Environ.*, 2006, **40**, 2690–2705.
26 R. Fisseha, M. Saurer and M. Jaggi, *Atmos. Environ.*, 2009, **43**, 431–437.
27 J. J. Cao, J. C. Chow, J. Tao, S. C. Lee, J. G. Watson, K. F. Ho, G. H. Wang, C. S. Zhu and Y. M. Han, *Atmos. Environ.*, 2011, **45**, 1359–1363.
28 K. M. Russel, J. N. Galloway, S. Macko, J. L. Moody and J. R. Scudlark, *Atmos. Environ.*, 1998, **32**, 2453–2465.
29 Y. Gao, *Atmos. Environ.*, 2002, **36**, 5783–5794.
30 S. G. Yeatman, L. J. Spokes, P. F. Dennis and T. D. Jickells, *Atmos. Environ.*, 2001, **35**, 1307–1320.
31 D. Widory, *Atmos. Environ.*, 2007, **41**(11), 2382–2390.
32 X. H. Bi, B. R. T. Simoneit, G. Sheng and J. Fu, *Fuel*, 2008, **87**, 112–119.
33 Z. F. Ren, X. H. Bi, B. Huang, M. Liu, G. Y. Sheng and J. M. Fu, *Environ. Pollut.*, 2013, **177**, 71–77.
34 X. H. Bi, S. L. Wei, B. Huang, M. Liu, G. Y. Sheng and M. Fu, *Atmos. Res.*, 2012, **109–110**, 76–83.
35 W. L. Ma, Y. F. Li, H. Qi, D. Z. Sun, L. Y. Liu and D. G. Wang, *Chemosphere*, 2010, **79**, 441–447.
36 S. Tao, Y. Wang, S. Wu, S. Liu, H. Dou, Y. Liu, C. Lang, F. Hu and B. Xing, *Atmos. Environ.*, 2007, **41**, 9594–9602.
37 W. L. Ma, D. Z. Sun, W. G. Shen, M. Yang, H. Qi, L. L. Yan, J. M. Shen and Y. F. Li, *Environ. Pollut.*, 2011, **159**, 1794–1801.
38 Y. J. Chen, Y. L. Feng, S. C. Xiong, D. Y. Liu, G. Wang, G. Y. Sheng and J. M. Fu, *Environ. Monit. Assess.*, 2011, **172**, 235–247.
39 Y. Wu, Y. Liu, X. Zheng, S. J. Zhang, S. J. Song, J. Q. Li and J. M. Hao, *Sci. Total Environ.*, 2014, **470–471**, 76–83.
40 X. F. Huang, L. Y. He, M. Hu and Y. H. Zhang, *Atmos. Environ.*, 2006, **40**, 2449–2458.
41 M. Fang, M. Zheng, F. Wang, K. L. To, A. B. Jaafar and S. L. Tong, *Atmos. Environ.*, 1999, **33**, 783–795.
42 W. F. Rogge, L. Hildemann, M. A. Mazurek, G. R. Cass and B. R. T. Simoneit, *Environ. Sci. Technol.*, 1993, **27**, 1892–1904.
43 G. D. Thurston and J. D. Spengler, *Atmos. Environ.*, 1985, **19**, 9–25.
44 M. F. Simcik, S. J. Eisenreich and P. J. Lioy, *Atmos. Environ.*, 1999, **33**, 5071–5079.
45 N. Yassaa, B. Y. Meklati, A. Cecinato and F. Marino, *Atmos. Environ.*, 2001, **35**, 1843–1851.
46 K. Ravindra, R. Sokhi and R. V. Grieken, *Atmos. Environ.*, 2008, **42**, 2895–2921.
47 C. Alves, C. Pio and A. Duarte, *Atmos. Environ.*, 2001, **35**(32), 5485–5496.
48 Z. G. Guo, T. Lin, G. Zhang, L. M. Hu and M. Zheng, *J. Hazard. Mater.*, 2009, **170**, 888–894.
49 J. L. Feng, C. K. Chan, M. Fang, M. Hu, L. Y. He and X. Y. Tang, *Chemosensors*, 2005, **61**, 623–632.
50 W. X. Liu, H. Dou, Z. C. Wei, B. Chang, W. X. Qiu, Y. Liu and S. Tao, *Sci. Total Environ.*, 2009, **407**, 1436–1446.
51 R. J. Huang, Y. L. Zhang, C. Bozzetti, K. F. Ho, J. J. Cao, Y. M. Han, K. R. Daellenbach, J. G. Slowik, S. M. Platt, F. Canonaco, P. Zotter, R. Wolf, S. M. Pieber, E. A. Bruns, M. Crippa, G. Ciarelli, A. Piazzalunga, M. Schwikowski, G. Abbaszade, J. Schnelle-Kreis, R. Zimmermann, Z. S. An, S. Szidat, U. Baltensperger, I. El Haddad and A. S. H. Prevot, *Nature*, 2014, **514**, 218–222.
52 W. Wang, T. Primbs, S. Tao, T. Zhu and S. L. M. Simonich, *Environ. Sci. Technol.*, 2009, **43**, 5314–5320.
53 J. Zhou, T. Wang, Y. Zhang, N. Zhong, P. Medeiros and B. Simoneit, *Atmos. Res.*, 2009, **93**, 849–861.
54 H. Kawashima and Y. Haneishi, *Atmos. Environ.*, 2012, **46**, 568–579.
55 I. Mori, M. Nishikawa, H. Quan and Y. Iwasaka, in *Abstract of Annual Meeting of Japan Society for Atmos. Environ*, 1999, vol. 40, p. 419.
56 H. Kawashima and Y. Haneishi, *Atmos. Environ.*, 2012, **46**, 568–579.
57 G. Liu, Q. Yao and H. Yang, *J. Environ. Health*, 2008, **25**, 822–823 (in Chinese).
58 J. D. Court, R. J. Goldsack, L. M. Ferrari and H. A. Polach, *Clean Air*, 1981, 6–11.
59 J. S. Nina, Y. Yang, C. Kuang, C. Fahe, C. Yizhen, W. Shulan and N. Stefan, *Urban Environ*, 2013, pp. 263–270.
60 H. Y. Xiao and C. Q. Liu, *Org. Geochem.*, 2011, **42**(1), 84–93.
61 T. H. E. Heaton, *Tellus*, 1990, **42**, 304.
62 T. Ancelet, P. K. Davy, W. J. Trompetter, A. Markwitz and D. C. Weatherburn, *Atmos. Environ.*, 2011, **45**(26), 4463–4469.
63 F. Lu, Z. Liu and H. Ji, *Sci. China: Earth Sci.*, 2013, **56**(2), 217–227.